PHYSICAL REVIEW B VOLUME 43, NUMBER 7 1 MARCH 1991

Properties of the 800-nm luminescence band in neutron-irradiated magnesium oxide crystals

R. Gonzalez* and Y. Chen
Solid State Division, Oak Ridge National Laboratory, Oak Ridge, Tennessee 37831-6031

R. M. Sebek, G. P. Williams, Jr., and R. T. Williams
Department of Physics, Wake Forest University, Winston-Salem, North Carolina 27109

W. Gellermann
Department of Physics, University of Utah, Salt Lake City, Utah 84101
(Received 1 August 1990)

We present results on the luminescence at 800 nm which occurs upon excitation of the 573-nm optical absorption band attributed to an aggregate defect in neutron-irradiated MgO crystals both pure and doped. The study was undertaken to evaluate the suitability of this luminescence for a tunable laser. Absorption, luminescence, and excitation spectra were measured before and after isochronal annealing, with the goal of optimizing the luminescence intensity and stability of the responsible defect, and reducing the background absorption in the crystal. The emission intensity is highest after annealing at ~550 K independent of dose. A thermally induced absorption band at 565 nm, which emerges at ~550 K, does not contribute to the emission at 800 nm. Under low-intensity continuous excitation, the 573-nm absorption band is not susceptible to photoconversion. However, when pumped with high-intensity laser light, the band exhibits a decay which recovers within 0.5 s. The luminescence has a single-exponential decay time of 15.5 ns at room temperature, and the band shape remains essentially constant throughout the decay. Tests for laser action using pulsed and cw pump lasers were unsuccessful at 77 and 300 K.

I. INTRODUCTION

The irradiation of undoped MgO single crystals by energetic neutrons ($E > 0.1$ MeV) produces several optically detectable defects: (1) anion vacancies (primarily the one-electron F^+ center) which absorb at about 250 nm (5.0 eV),[1,2] (2) anion divacancies which absorb at 975 and 355 nm (1.3 and 3.5 eV, respectively),[3-6] and (3) an unidentified aggregate defect which absorbs at 573 nm (2.2 eV).[1,6-8] The 573-nm band, whose full width at half maximum (FWHM) is 0.3 eV, should not be confused with the 540-nm (2.3-eV) band, which is due to trapped-hole defects.[9,10] The latter is broader (FWHM = 1.1 eV) and decays in a few days at room temperature. The energy dependence of electron irradiation indicates that production of defects responsible for the 573-nm band has a relatively low threshold energy, compatible with two adjacent vacancies.[11] However, it is not a simple anion divacancy and is not paramagnetic. The absorption of light in the 573-nm band yields a near-infrared luminescence at 800 nm (1.55 eV).[12] This luminescence can be quite intense.

The present study focuses on the effect of thermal annealing on the 573-nm absorption band and on the intensity of the 800-nm luminescence band. The motivation for the study is that a strong luminescence band could be the basis for a solid-state tunable laser, providing the efficiency could be maximized, the background and parasitic absorption minimized, and the spontaneous lifetime is favorable with no significant ionization from the excited state. For comparison, parallel experiments were performed on a crystal doped with hydrogen and one doped with lithium, referred to as MgO:H and MgO:Li, respectively. The former is intriguing because hydrogen is a persistent impurity in MgO, and is known to dominate electron trapping and recombinations at F centers. The latter is of interest because the production of intrinsic point defects by neutron bombardment is inhibited by the presence of lithium.[13] In particular, the 573-nm band is reduced by a factor of 6.

II. EXPERIMENTAL PROCEDURES

All the MgO crystals used in this work were grown by the arc-fusion method. Undoped crystals were grown by a variation of this technique which gives larger and clearer crystals of high purity.[14] The starting material was high-purity MgO powder from the Kanto Chemical Company, Tokyo, Japan. Typical chemical analyses have been reported previously.[11] The hydrogen-doped MgO crystals were grown by presoaking the MgO powder with water. Lithium doping was achieved by mixing 5% of Li_2CO_3 powder with the MgO powder before the crystal growth. The lithium concentration in the resulting crystals was determined to be approximately 0.03 at.%.[15] Neutron irradiations were performed at the Oak Ridge National Laboratory National Low Temperature Neutron Irradiation Facility, using fluxes of 2×10^{13} fission spectrum neutrons/cm^2 s ($E > 0.1$ MeV). The neutron dose varied between 2×10^{17} and 7×10^{18} neutrons/cm^2.

The samples were cooled in flowing helium gas. The ambient temperature was about 320 K.

Isochronal annealing in 15-min stages with increasing temperature was performed in flowing nitrogen using a Lindberg 5400 series furnace. Near-infrared, visible and ultraviolet measurements were made with a Perkin-Elmer Lambda 9 spectrophotometer. The excitation and luminescence spectra were taken with a Spex Industries Fluorometer, Model 212, using a cooled Hamamatsu R928 photomultiplier tube. The spectra were corrected for the response of the photomultiplier tube. Bleaching experiments were made with a 1000-W xenon lamp used in conjunction with a 0.125-m monochromator. The spectral band pass was about 15 nm.

Time-resolved measurements were made by exciting with 575-nm dye laser pulses of 3-ns duration, and measuring the luminescence spectra with a gated optical multichannel analyzer. The time resolution of the luminescence decay plots is limited by the 10-ns gate width of the microchannel plate intensifier.

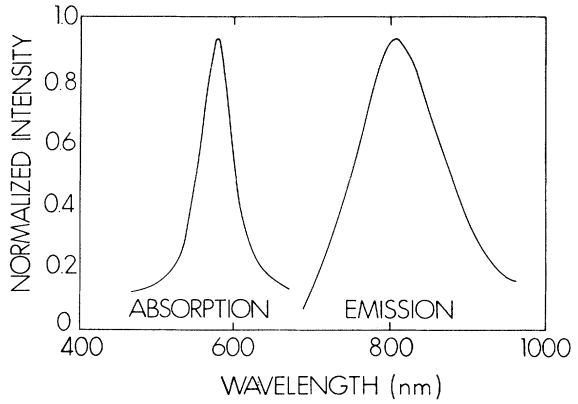

FIG. 1. Optical spectra of a neutron-irradiated MgO crystal illustrating the absorption band at 573 nm and the emission band at 800 nm resulting from excitation in the absorption band.

III. RESULTS

Four undoped MgO samples were neutron irradiated to different doses, while the MgO:H and MgO:Li crystals received the same dose, as shown in Table I. After neutron irradiation, the samples exhibited the bands at 250, 355, 573, and 975 nm, with the exception of the MgO:Li sample, which exhibited a band at 235 nm but not at 250 nm. The latter band has been attributed[16] to an anion vacancy perturbed by two Li^+ ions, having a linear configuration along a $\langle 100 \rangle$ direction: $O^{2-}-Li^+-$(oxygen vacancy)$-Li^+-O^{2-}$. In all the samples, excitation of the 573-nm band produced luminescence at 800 nm (see Fig. 1). Absorption, luminescence, and excitation measurements were made before and after each isochronal anneal for all six samples, in order to establish the general behavior of the 573-nm band and the 800-nm luminescence.

A. Absorption measurements

Figure 2 shows the optical absorption spectra of the as-irradiated MgO sample *B* (dose $=1.7\times10^{18}$ n/cm^2, low hydrogen content) before and after subsequent anneals at 530, 730, and 830 K. Thermal treatment not only changed the shape and intensity of the absorption bands, but also annealed out much of the background absorption and scattering loss due to the neutron bombardment. Such a broad absorption spectrum with scattering losses extending down below the short-wavelength region is typical of neutron damage and is a significant problem when color-center lasers in neutron-irradiated crystals are contemplated. Figure 2 shows that annealing significantly reduces the background losses. Annealing at 530 K or above practically eliminates the background absorption underlying the luminescence at 800 nm. The absorption at 573 nm is plotted as a function of isochronal annealing temperature (solid curve) in Fig. 3. The absorption decreased monotonically with successive thermal treatment until 600 K; it then increased and reached a peak at about 720 K before decreasing rapidly thereafter. Above

TABLE I. Neutron doses for four undoped and two doped MgO crystals.

Sample	Thickness (mm)	Dose (n/cm^2)
MgO *A*	3.0	3.0×10^{17}
MgO *B*	3.1	1.7×10^{18}
MgO *C*	6.9	1.1×10^{18}
MgO *D*	1.3	6.9×10^{18}
MgO:H	2.7	2.2×10^{17}
MgO:Li	1.6	2.2×10^{17}

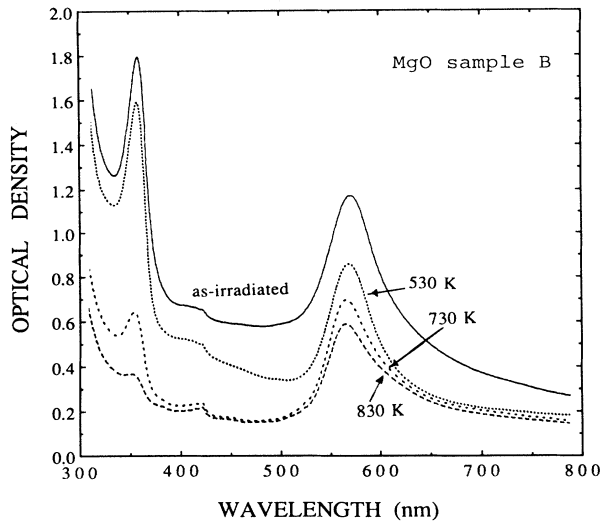

FIG. 2. Optical absorption spectra of MgO sample *B*, irradiated to a dose of 1.7×10^{18} n/cm^2 measured before and after ischronal annealing at 530, 730, and 830 K. A shift of the composite band peak to lower wavelengths after the annealing can be discerned.

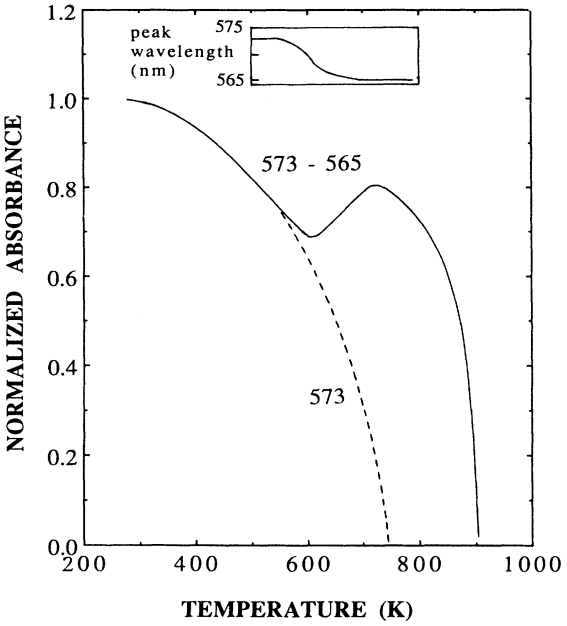

FIG. 3. Absorption at 573 nm vs annealing temperature for MgO sample *B*. The change in peak wavelength from 573 to 565 nm with annealing temperature is plotted in the inset.

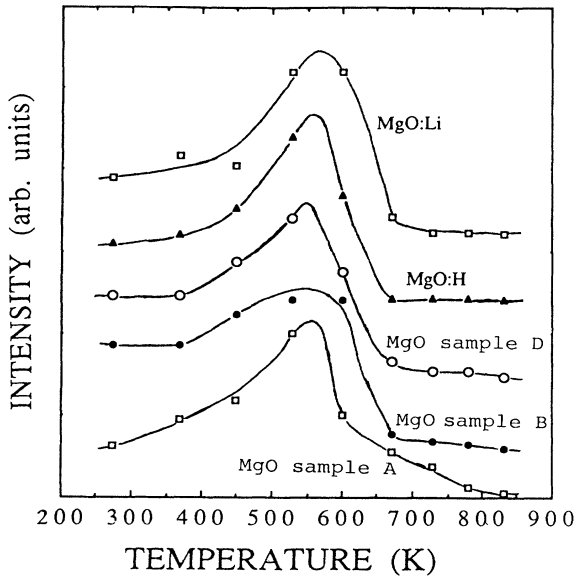

FIG. 4. Luminescence intensity measured at 750 nm vs isochronal annealing temperature for five neutron-irradiated samples, including MgO:H and MgO:Li. Excitation is at 573 nm.

900 K it virtually vanished. In the anneals above 550 K, the absorption at 573 was composed of at least two bands, as reported earlier:[8] one peaked at 573 nm and the other at 565 nm. One indicator was that above 550 K the peak of the composite bands began to shift toward 565 nm (see inset in Fig. 3). Above 700 K the peak occurred at 565 nm, indicating that the 573-nm absorption band had practically vanished.

B. Luminescence and excitation measurements

The intensity of the 800-nm emission band is plotted in Fig. 4 as a function of the annealing temperature for five of the samples. The curves were similar and were characterized by an intensity maximum after annealing at 550 K. Also, the same 573-nm absorption and 800-nm emission bands were observed in all six crystals, independent of hydrogen or lithium doping. This observation, together with the similar annealing peaks in Fig. 4, is consistent with previous conclusions that the defect is intrinsic.[6,9,11]

Excitation spectra with the emission wavelength fixed at 750 nm were also obtained for all six crystals before and after each anneal. The results from MgO sample *A* are shown in Fig. 5. The wavelength of maximum excitation efficiency peaked at about 573 nm. Again, we note that the intensity reached a maximum after the 530-K anneal, confirming the results obtained from the absorption measurements.

The temperature-dependent emission curves shown in Fig. 4 present an interesting contrast with those of the temperature-dependent absorption at 573 nm, shown in Fig. 3. At 530 K the 573-nm absorption band has decreased 20%, but the emission intensity has increased threefold. After annealing at 600 K the absorption at 573 nm, due to the composite 573–565-nm bands, decreased 30%, but the emission was still more intense than in the as-irradiated state. Between 600 and 800 K, the emission intensity decreased rapidly while the absorption at 573 nm was actually higher.

In order to evaluate the quantum efficiency of the 800-nm emission, the luminescence for MgO sample *D* after annealing at 530 K was measured at 77 and 295 K. The intensity at 77 K was ~20% higher, which suggests a high quantum efficiency.

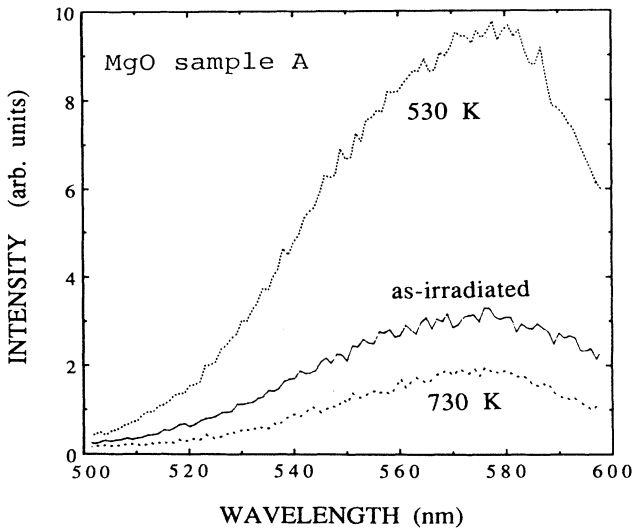

FIG. 5. Excitation spectra for MgO sample *A* with the emission wavelength set at 750-nm before and after isochronal annealing at 530 and 730 K.

C. Photobleaching in the steady state

To determine whether the 573-nm band was susceptible to photoconversion under excitation, MgO sample *C* was annealed at 543 K for 15 min and then photobleached with 573-nm light for 5 h at room temperature. The results are shown in Fig. 6. It is evident that the absorption band remained intact and showed no sign of photoconversion.

D. Time-resolved spectroscopy

Figure 7 shows the decay of the 800-nm luminescence following 3-ns pulsed excitation with 575-nm light. The initial response appeared rounded because of the 10-ns gate width at the detector. Thereafter, the decay is nearly a straight line on the semilog plot of Fig. 7, indicating a single exponential decay with $\tau = 15.5$ ns over the three decades plotted. There was no evidence of a long phosphorescence tail. In order to verify that a single-defect state was responsible for the 800-nm luminescence throughout its decay, we measured the luminescence spectra with successive delays; this is shown in Fig. 8. The spectra were corrected for wavelength response of the detector. The apparent intensity increase at 900 nm is an artifact of the vastly diminished detector sensitivity. We are convinced that the 800-nm band shape remained constant throughout its decay.

E. Testing for laser action

For the laser experiments we tested two samples, 2.0- and 4.4-mm thick, which were irradiated to 2.2×10^{17} neutron/cm^2 and annealed at 560 K. The absorption spectrum of the thicker sample is shown in Fig. 9, revealing an absorption coefficient of 5 cm^{-1} for the 573-nm band and 1.5 cm^{-1} for an absorption band at 975 nm.

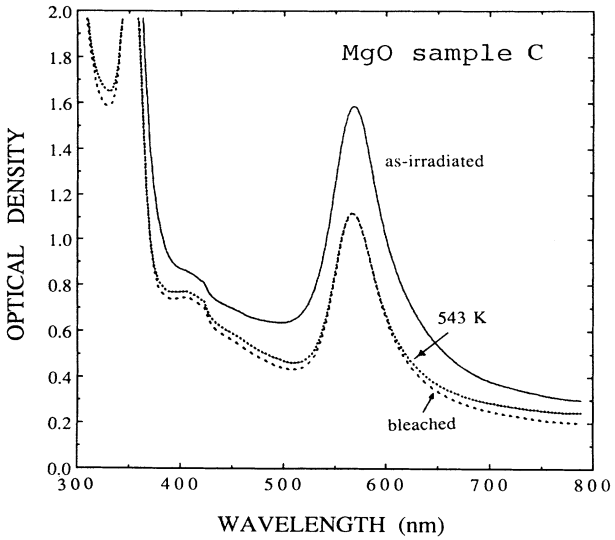

FIG. 6. Results of photo-excitation of the 573-nm absorption band in MgO sample *C* for 5 h following neutron irradiation to a dose of 1.1×10^{18} n/cm^2, and subsequent annealing at 543 K.

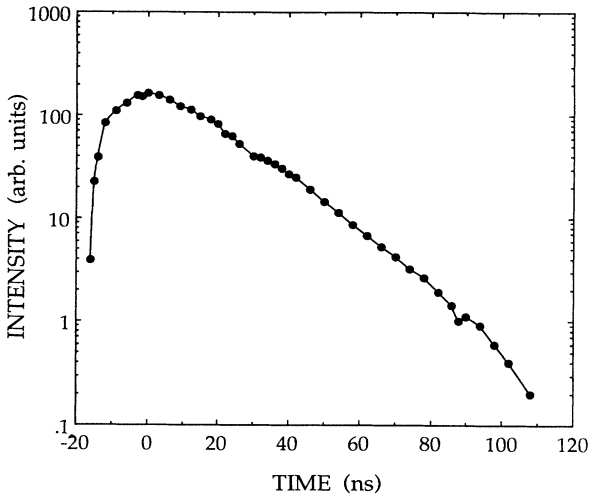

FIG. 7. Decay of the 800-nm luminescence following 3-ns pulsed excitation with 575-nm light room temperature. The zero of time represents coincidence of the excitation pulse and the center of the 10-ns detector gate width.

For the fluorescence peak at 800 nm, where the laser transition is expected to occur, the loss per pass from absorption and scattering is about 17%.

The laser cavity consisted of an x-shaped astigmatically compensated four-mirror configuration (Fig. 10) employing a dichroic plane input coupler (with high transmission at 580 nm, and high reflectivity at 780 nm), two highly reflective silver-coated folding mirrors (75-mm radius of curvature), and a plane output coupler (96% reflection at 780 nm). The crystal was in thermal contact with a liquid nitrogen Dewar and was oriented at Brewster's angle. The pump laser was focused by one of the folding mirrors into a diffraction-limited ~10-μm diameter spot inside the crystal.

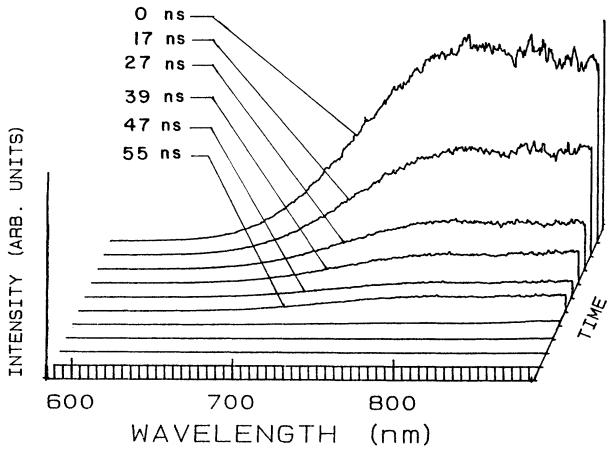

FIG. 8. Successive luminescence spectra measured at the indicated time delays following excitation by a 3-ns pulse of 575-nm light.

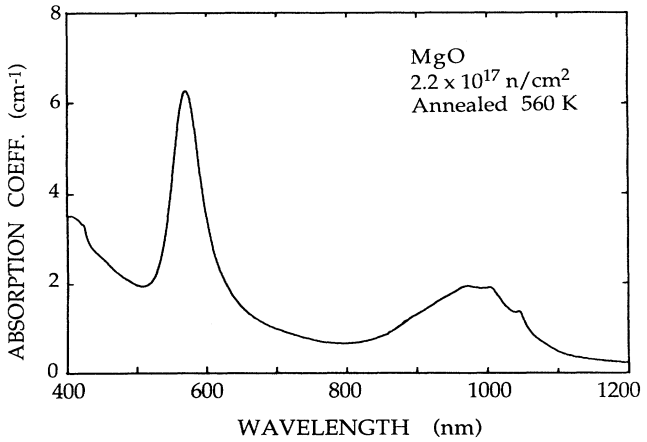

FIG. 9. Absorption spectrum of the 4.4-mm thick sample used in laser test described in the text.

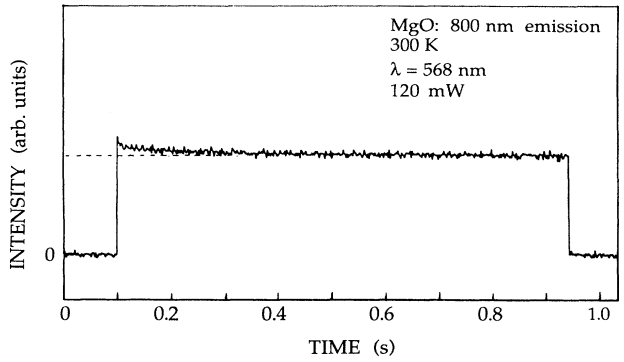

FIG. 11. Emission intensity at 800 nm as a function of time under stepwise laser excitation at 568 nm (120 mW) showing ~16% fading of the emission from its initial value within ~0.5 s.

Prior to the MgO laser experiments, the cavity was tested and aligned by operating it with a 647-nm pumped LiF:F_2^+ color center laser (laser transition at ~900 nm). After that test, only the input and output coupling mirrors were changed for MgO fluorescence, while the optimized folding mirror spacing remained unchanged.

We used both cw- and pulsed-laser sources to pump the 573-nm band. The cw pump laser was a krypton laser operating at the 568-nm line with ~800 mW maximum available pump power; the pulsed laser was an excimer laser-pumped dye laser (Coumarin 153), operating in the yellow/green range with 15-ns pulse width and pulse power up to the MW range.

Laser oscillation of the MgO crystal could not be obtained at 300 or 77 K with either of the two pump sources. In the case of the pulsed excitation, care had to be taken to use a sufficiently low pump power to avoid surface damage of the pumped crystal spot. With a higher repetition rate (20 Hz) of the pulsed excitation and the cw excitation, a fading of the fluorescence was observed. Using the maximum 568-nm pump power of ~800 mW, ~20% of the fluorescence intensity faded within a fraction of a second after a "fresh" crystal spot was selected. This fading behavior is shown quantitatively for reduced pump power levels (120 mW) at 300 K in Fig. 11. Following "step-function excitation" (realized with an acoustic-optic modulator switch), the fluorescence intensity fades nonexponentially from its initial level to a ~84% level within ~0.5 s.

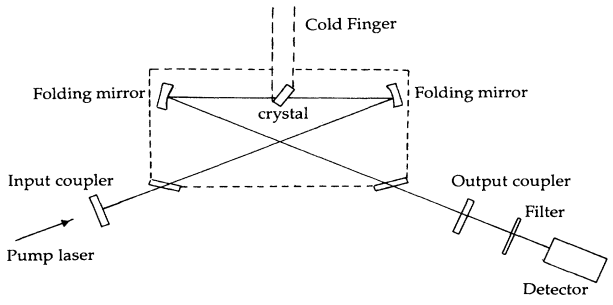

FIG. 10. Schematics of the astigmatically compensated four-mirror-resonator configuration used for the tests are described.

IV. DISCUSSION AND CONCLUSIONS

The present study has focused on the absorption band at 573 nm in neutron-irradiated MgO and its emission at 800 nm. Four undoped samples irradiated to different doses and two doped crystals (MgO:H and MgO:Li) irradiated to a lower dose, were examined. The following general observations were made: first, thermal treatment to reduce background losses diminished the absorption band at 573 nm, but began to create a band at 565 nm at $T=550$ K. This thermally generated absorption band vanished rapidly above 800 K. Second, the dependence of emission intensity on annealing temperature was similar for all the samples, with a maximum occurring at 550 K, as noted in Fig. 4. The maximum intensity at 550 K was independent of neutron dose, and of hydrogen and lithium dopants. Third, the excitation spectra indicate that the peak excitation wavelength coincided with the absorption peak at 573 nm and that the intensity was largest after anneals at 550 K.

These observations permit us to describe the cause of the peak emission efficiency at 550 K. Energetic neutrons create severe lattice damage, which we believe is primarily responsible for the initial low-luminescence intensity as a result of various quenching mechanisms. Thermal treatment anneals the damage. Therefore, one can expect an increase of the luminescence intensity after thermal treatment, and an increase was observed up to 550 K. However, the rather rapid decrease in intensity above this temperature cannot be attributed to the change of absorption at 573 nm. We propose that the declining intensity for temperatures above 550 K was caused by the emergence of the 565-nm absorption band which competes with the 573-nm band for photons but does not emit at 800-nm. From the three temperature-dependent curves, namely the absorption (Fig. 3), the peak wavelength (Fig. 3, inset) and the emission intensity (Fig. 4), we deduce

that the 565-nm absorption band becomes predominant above 700 K, and at 800 K the 573-nm band is virtually nonexistent. We illustrate our projection of annealing the 573-nm band by the dotted curve shown in Fig. 3.

It is evident that to maximize the luminescence intensity at 800-nm, it is necessary to anneal the neutron-irradiated samples at 550 K. At this temperature the lattice damage cause by neutron bombardment relaxes sufficiently such that a high quantum efficiency is obtained.

Measured spontaneous lifetime can be used to estimate the stimulated emission cross section σ for this defect:

$$\sigma = \frac{\lambda_0^2 \eta}{\delta \pi \eta^2 (\Delta \nu) \tau} , \quad (1)$$

where η is the quantum efficiency, λ_0 the peak wavelength of the band, $\Delta\nu$ the full width at half maximum, and τ the luminescence lifetime. Using $\lambda_0 = 0.80$ μm, $\tau = 15.5$ ns, $\Delta\nu = 5.55 \times 10^{13}$ Hz (0.23 eV) and assuming $\eta = 1$, the cross section σ is found to be 8.9×10^{-17} cm^2. To evaluate the likelihood of achieving laser oscillation, we use the cross section to predict the inversion threshold N_t^*, and then compare the achieved inversion, N_a^*, under the pump conditions described. The threshold inversion is given by

$$N_t^* = \frac{L + T}{z\sigma} . \quad (2)$$

Here, Z is the gain length (crystal thickness), L the internal (single pass) loss factor, and T the output coupling. Using $z = 0.2$ cm, $\sigma = 8.9 \times 10^{-17}$ cm^2, $L + T \approx 0.25$, N_t^* becomes 1.4×10^{16} cm^{-3}.

This value has to be compared with the population N_a^* actually achieved in the laser experiments. Assuming that each pump photon excites a defect to the upper laser transition and that this defect behaves as a four-level system, this population can be estimated for steady-state conditions from the relation

$$N_a^* = \frac{I \alpha \tau}{E} , \quad (3)$$

where α is the absorption coefficient at the pump wavelength, I the pump intensity in the cavity beam waist, E the pump photon energy, and τ the lifetime of the emission. Using $\alpha = 4.5$ cm^{-1} (compare Fig. 9), $I = 800$ mW per beam waist area $A \sim 2.2 \times 10^{-6}$ cm^2, $E = 2.18$ eV, and $\tau = 15.5$ ns, we obtain $N_a^* = 7.3 \times 10^{16}$ cm^{-3}. Since $N_a^* > N_t^*$, laser oscillation should have been possible if all the assumptions made above were realized in this system.

However, since laser oscillation could not be obtained, we conclude that these assumptions are not fulfilled. The reasons may include the following. (1) The quantum efficiency η may be lower than the assumed value of unity and (2) additional loss mechanisms, such as excited-state absorption, may be present in the optical pumping cycle. By using Smakula's equation and assuming that the oscillator strength in absorption is $f = 0.5$, the ground-state (unpumped) defect concentration in our sample is found to be 2.6×10^{16} cm^{-3}. This is barely larger than the threshold population inversion N_t^* required under the best of circumstances ($\eta = 1$). On the basis of the above estimates, we believe that this system is marginal at present. Barring significant excited-state absorption, a factor of 3 or 4 improvements of one or a combination of the following parameters should result in a laser: increase in the efficiency η, increases of defect concentration, and hence of absorption coefficient α in Eq. (3), and decrease in the internal loss L at 800 nm. The photobleaching observed at high-pump intensity will also have to be controlled for a practical laser.

ACKNOWLEDGMENTS

The authors gratefully acknowledge M. M. Abraham, who assisted in the growth of the high-purity MgO crystals. This research was sponsored by the Defense Advanced Research Projects Agency under Interagency Agreement 40-1611-85 with Martin Marietta Energy Systems, Inc., Contract No. DE-AC05-84OR21400 with the U.S. Department of Energy, and the National Science Foundation Grant No. DMR 87-06416. One of us (R.G.) wishes to acknowledge the support of the Comisión Asesora de Investigación Científica y Técnica of Spain.

*Permanent address: Departamento de Física del Estado Sólido, Facultad de Ciencias Fisicas, Universidad Complutense, 28040 Madrid, Spain.

[1]Y. Chen, J. L. Kolopus, and W. A. Sibley, Phys. Rev. B **25**, 2077 (1969).

[2]L. A. Kappers, R. L. Kroes, and E. B. Hensley, Phys. Rev. **1**, 4151 (1970).

[3]I. K. Ludlow and W. A. Runciman, Proc. Phys. Soc. (London) **86**, 1081 (1965).

[4]I. K. Ludlow, Proc. Phys. Soc. (London) **88**, 763 (1966).

[5]B. Henderson and J. E. Wertz, Adv. Phys. **17**, 749 (1968).

[6]Y. Chen, R. T. Williams, and W. A. Sibley, Phys. Rev. **182**, 960 (1969).

[7]B. Henderson and R. D. King, Philos. Mag. A **13**, 1149 (1966).

[8]Y. Chen and W. A. Sibley, Philos. Mag. A **20**, 217 (1969).

[9]A. E. Hughes and B. Henderson, in *Defects in Crystalline Solids,* edited by J. H. Crawford, Jr. and L. M. Slifkin (Plenum, New York, 1972), and references therein.

[10]M. M. Abraham, J. L. Boldu, and Y. Chen, in *Electron Magnetic Resonance of the Solid State,* edited by John A. Weil (Canadian Society for Chemistry, Ottawa, Canada, 1987).

[11]Y. Chen, D. L. Trueblood, O. E. Schow, and H. T. Tohver, J. Phys. C **3**, 2501 (1970).

[12]Y. Chen, J. L. Kolopus, and W. A. Sibley, J. Lumin. H **4**, 633 (1970).

[13]Y. Chen and M. M. Abraham, J. Am. Ceram. Soc. **59**, 101 (1976).

[14]M. M. Abraham, C. T. Butler, and Y. Chen, J. Chem. Phys. **55**, 3752 (1971).

[15]J. Narayan, M. M. Abraham, Y. Chen, and H. T. Tohver, Philos. Mag. A **38**, 247 (1978).

[16]Y. Chen, M. M. Abraham, J. L. Boldu, and V. M. Orera, J. Phys. (Paris) Colloq. **41**, C6-398 (1980).